European Journal of Pharmaceutics and Biopharmaceutics 142 (2019) 344–352

Contents lists available at ScienceDirect

European Journal of Pharmaceutics and Biopharmaceutics

journal homepage: www.elsevier.com/locate/ejpb

Research paper

How to measure coating thickness of tablets: Method comparison of optical coherence tomography, near-infrared spectroscopy and weight-, height- and diameter gain

P.R. Wahl[a], A. Peter[a], M. Wolfgang[a], J.G. Khinast[a,b,*]

[a] Research Center Pharmaceutical Engineering GmbH, Inffeldgasse 13/2, 8010 Graz, Austria
[b] Institute for Process and Particle Engineering, Graz University of Technology, Inffeldgasse 13/3, 8010 Graz, Austria

ARTICLE INFO

Keywords:
Film coating
Coating variability
Optical coherence tomography (OCT)
Near-infrared spectroscopy (NIR)
Process analytical technology (PAT)

ABSTRACT

Film coating of pharmaceutical dosage forms, such as tablets and pellets, can be used to tailor the drug release profile. With that regard, a uniform coating thickness of a single tablet (*intra*-tablet), all tablets (*inter*-tablet) and subsequent batches (*inter*-batch) is crucial. We present a method comparison between in-line (optical coherence tomography and near-infrared spectroscopy) and well-established off-line (height-, weight- and diameter-gain) approaches to determining the coating thickness of tablets. We used single tablets drawn during a commercial coating process. Comparing the low *intra*- and high *inter*-tablet coating variability indicated that the tablets had a broad distribution of spray zone passes but at a random tablet orientation. Even at the end of the coating process at a mean coating thickness of about 70 µm, the *inter*-tablet standard deviation was about 9 µm or 13% relative standard deviation. Determining correlations between the methods identified the factors that contribute to the measurement uncertainty and bias for each method. Ultimately, we aimed to establish that in-line methods match or even surpass the conventional off-line reference methods in terms of accuracy and precision of coating thickness measurement.

1. Introduction

Coating of oral solid dosage forms, such as tablets and pellets, is an important unit operation in pharmaceutical manufacturing, since it can be used to define the release profile of the active pharmaceutical ingredient (API). There are three main coating types of API release behavior, i.e., (1) immediate release, (2) modified release and (3) controlled or sustained release [1]. Immediate release coatings often serve cosmetic purposes (e.g., brand, dosage strength identification) or compliance purposes (e.g., taste masking, easier swallowing). In this case, the coating thickness is of low biopharmaceutical importance. Modified-release coatings are typically applied to resist the gastric juices (enteric coating). Proper functionality requires a coating that is above a minimum thickness with a low *inter*-tablet coating thickness variability. Controlled- or sustained-release coatings ensure a defined release profile of the drug over an extended period of time. In diffusion-based coatings [2] and osmotic systems [3,4] the coating thickness and variability (*intra*- and *inter*-tablet) are thus critical quality attributes [5,6]. The release profile depends not only on the coating thickness but also on the porosity of the polymeric film and its evolution during dissolution, on the surface area and on the added (in-)soluble excipients [7–9].

Several modelling efforts aimed at gaining a mechanistic understanding of the release profile, which have to be validated based on experimental observations [7], such as the evolution of microstructure and its effect on the diffusion coefficients [8]. A faster release rate is commonly accomplished via thinner coatings, increased coating porosity or larger total surface area. Significantly slower release rates may be achieved by incorporating impermeable objects, e.g., inorganic particles, crystallites or nanoclays [9]. Thus, in addition to the coating thickness and its variation, the microstructure needs to be considered.

Due to the numerous formulation and processing factors influencing the performance of functional coatings, development and manufacturing of coated dosage forms is challenging [10]. Currently the scale-up and transfer to manufacturing equipment is strongly based on experience and utilizing dimensionless numbers for the equipment. This approach needs to imply that the coating structure and coating thickness uniformity remains the same, because such measurements are not accessible, or are very time consuming. Ultimately, the dissolution test will determine if a process transfer was successful. Here, OCT can help

* Corresponding author at: Institute for Process and Particle Engineering, Graz University of Technology, Inffeldgasse 13/3, 8010 Graz, Austria.
E-mail address: khinast@tugraz.at (J.G. Khinast).

https://doi.org/10.1016/j.ejpb.2019.06.021
Received 29 March 2019; Received in revised form 24 May 2019; Accepted 18 June 2019
Available online 02 July 2019
0939-6411/

to generate knowledge if and how the formulation and process parameters affect the coating properties, and how these in turn affect the quality attributes, e.g. dissolution. Measuring the coating parameters during each step of pharmaceutical development thus supports a more streamlined scale-up.

Tablet coating is commonly performed in perforated pan coaters [11]. The coating uniformity is influenced by the equipment geometry (e.g., the baffle design), the coating solution properties (e.g., the solid content, viscosity and surface tension) and a multitude of process parameters (e.g., the spray rate, inlet air temperature and relative humidity, bed temperature, pan radial velocity, atomizing and pattern air pressure, orientation of nozzles, distance to tablet bed and number of nozzles) [6,12–14]. These parameters influence the spray pattern on the tablet bed surface, the particle size distribution of droplets, the drying of spray droplets before they hit the tablets and the thermodynamics of drying. Optimizing the coating process should be supported by CFD/DEM simulations. Though based on first principle calculations, such models still have a few fitting parameters. To identify these parameters and to validate the simulations, reliable and fast in-line reference measurements are required. Additionally, parallel in-line measurements can help to determine potential influencing factors not considered by the model.

Several in-line methods have been utilized to study the coating growth on pharmaceutical pellets and tablets. These include near-infrared (NIR) [15–19] and Raman spectroscopy [20,21], terahertz pulsed imaging (TPI) [22,23], visual imaging [24,25] and optical coherence tomography (OCT) [22,26,27]. A detailed review was published by Knop et al. [1].

NIR and Raman spectroscopy are indirect methods that measure the intensity of spectral fingerprints of NIR/Raman active compounds in the illuminated or sampled volume. The sample volume depends on the penetration depth of radiation, which is material and wavelength-specific [28]. It is influenced by the material's absorption peaks and scattering properties defined by the particle size distribution (PSD), shape and surface roughness. Additionally the contribution to the overall NIR signal is not the same throughout the sample volume [29]. The spectral information can be correlated to coating thickness only by using chemometric models. NIR can acquire the spectra significantly faster than Raman, in the low millisecond range, which allows to measure single tablets in-line. The Raman signal, in contrast, is less influenced by water due to its low Raman scattering coefficient (i.e., the influence of residual moisture is expected to be lower than in NIR). However, RAMAN measurements take longer and thus, yield integral values of coating properties.

OCT and TPI directly measure the optical path length of the coating layer. Thus, a simpler referencing based on determining the refractive index of the examined material is possible. Due to a higher speed and resolution of OCT, coating as thin as about 10 µm can be measured. Additionally, information about the coating structure can be obtained, i.e., the *intra*-particle coating variability, distribution of coating particulates and properties of interface between the coating and the core. Due to longer wavelengths used, TPI can penetrate scattering coatings containing inorganic pigments and thicker layers, but it cannot resolve layers below 30 µm (measured on PE foils) [30] to 50 µm (measured on tablet coatings) [22].

Visual imaging can mainly be applied to pellet coating. It is a direct measurement of the entire particle size, including the coating and the core. Assuming a constant core particle size distribution, the average coating thickness and an estimate of its distribution can be calculated.

Our paper focusses on an experimental comparison of in-line OCT and NIR approaches to the established off-line height-, weight- and diameter-gain methods. Based on the experimental data obtained, contributions to the measurement uncertainty are analyzed. In addition, we aimed to test if the in-line methods match or even surpass the established off-line reference methods in terms of accuracy and precision.

2. Materials and methods

2.1. Materials

All sample tablets were drawn during a commercial manufacturing process. The cores were bi-convex tablets with an average weight of 200 mg and a dosage strength of 100 mg of a common pain killer. An enteric coating based on Eudragit L 30 D-55 30% aqueous dispersion (Evonik, Germany) with a target weight gain of 8% was applied in a perforated pan coater with a batch size exceeding 100 kg (Bohle, Germany). According to the confidentiality agreement with the manufacturer, the exact composition of coating and core cannot be disclosed.

2.2. Sampling and method comparison procedure

During the coating process, nine samples consisting of approx. 150 to 200 tablets each were drawn at 15, 45, 75, 105, 135, 165, 195, 225 and 240 min. The last sample at minute 240 corresponds to the target coating end-point of 8% weight gain. For each sample, 10 tablets were labelled to allow a direct tablet-by-tablet comparison. To mimic an in-line measurement, the entire sample was loaded into a miniature perforated drum for at-line measurement (OSeeT tablet sampling device, Phyllon, Austria). It consists of a small drum of 20 cm in diameter with a single line of perforations with 3 mm in diameter and a distance between perforation center points of 5 mm. The drum has adjustable rotational speed. The OCT probe was permanently mounted on the device, while the NIR probe was placed on a lab stand with clamp (with OCT probe removed). Both probes were installed in the same position outside of the drum directly below the center of the tablet bed at an angle of 45° from the vertical, to measure the tablets in the sampling device through the perforations. All samples were measured for 3 minutes at a rotational speed of 30 rpm.

2.3. Weight-, height- and diameter gain

The individual tablet weights were measured using a precision scale (XP205DR, Mettler Toledo USA, resolution 0.01 mg). Diameter and height measurements were performed with a micrometer screw gauge with torque control (QuantuMike MDE-25MJ, Mitutoyo Europe, Germany, resolution 1 µm). Three replicated measurements per tablet were performed and averaged to minimize the operator influences.

Based on the weight gain, the coating thickness was estimated. Therefor the density ρ of the dried coating formulation was calculated. The coating thickness x of the biconvex tablets was computed by numerically solving the equation

$$\begin{aligned} m_{\text{total}} &= m_0 + m_x \\ &= m_0 + \rho\pi((r+x)^2 s + (r+x)^2(h+x) + 3(h+x)^3 - (r^2 s + r^2 h \\ &\quad + 3h^3)) \end{aligned}$$

for x, with measured weight m_{total}, weight gain m_x, and tablet core properties weight m_0, = 196 ± 2 mg, radius$r$ = 4.044 ± 0.002 mm, dome height$h$ = 0.9 ± 0.008 mm and band height$s$ = 1.996 ± 0.008 mm. Ten tablet cores were measured. This equation assumes a uniform coating thickness over the entire tablet (0 µm *intra*-tablet coating variability).

2.4. Optical coherence tomography

Off-line investigations were performed via a 3D OCT setup (resolution: 4.1 µm axial in air, 10 µm lateral in focus, 1.6 mm image height in air), as described in [27]. For each tablet, a B-scan with 6.12 mm length consisting of 1024 A-scans was acquired from the top, bottom and band. For at-line measurements, a process OCT system with a 1D probe (OSeeT pharma 1D, Phyllon, Austria, resolution: 4.1 µm axial in air, 15 µm lateral in focus, 2.76 mm image height in air) was

used. Both systems employ a superluminescent diode (SLD) with a central wavelength of 830 nm and a bandwidth of 62 nm. The OCT image acquisition in the 3D system was accomplished via a custom software. The image acquisition in the 1D system and the evaluation of all OCT data were executed via the vendor software (OSeeT 3.3, Phyllon, Austria). The minimum coating thickness, below which measurements were discarded, was set to 12 µm. No additional data pretreatment or sorting was required.

Based on the OCT images, the following parameters were evaluated: the coating thickness per tablet, the standard deviation (SD) of coating thickness between the tablets, the surface roughness and the homogeneity index. Surface roughness *Rq* is calculated as the root mean square deviation of the detected surface versus an ellipse fit, as described in [31]. In the OSeeT software, the homogeneity index is given in percent and is defined as 100% minus the fraction of coating that appears dark in the OCT image due to reflections or scattering. This way, the area of regions (pixels) that are above a defined threshold can be compared to the entire coating area. We used a threshold of 0.1, of a range of 0 to 1 (white to black) and a minimum area of 5 connected pixels to suppress noise. This image analysis of homogeneity requires a minimum coating thickness of about 30 µm, based on the OSeeT system's axial resolution and analysis procedure.

2.5. Near-infrared spectroscopy

All measurements were performed using a process NIR spectrometer (SentroPAT FO, Sentronic, Germany, spectral resolution: 2 nm, 1100–2200 nm) with a probe of 6 mm spot size (SentroProbe DR LS). For off-line measurements of top and bottom, each tablet was placed directly on top of the probe window. The integration time for off-line measurement was set to 20 ms, with an averaging of 40 spectra, leading to a total integration time of 800 ms. For at-line measurement no averaging was performed, with a total integration time of 20 ms, to allow later spectral sorting and to obtain spectra mainly of single tablets. These spectra correspond to the mean coating thickness.

For at-line measurements potentially more than one tablet can contribute to the obtained spectrum, due to the drum geometry, the rotational speed of 30 rpm, 20 ms integration time and the 6 mm spot size. As the used NIR probe was a contact probe, the distance to the sample was important. Only tablets which were located directly behind the perforation provide sufficient backscattered signal intensity. The perforated drum was sprayed matte (flat) black to minimize specular reflections from the metal. That way the backscattered light from the tablet surface was the main contribution to the NIR spectrum. Additional spectra sorting was performed in order to remove all spectra with insufficient signal from tablets, e.g. due to a too large tablet-sensor distance or no tablet at all in the field of view. The criteria used for sorting was based on the intensities at specific wavelengths, $I_{1634\,nm} < I_{2030\,nm}$, due to which 81.1% of acquired spectra were dismissed.

2.6. Light microscopy

A light microscope (DM 4000M, Leica, Germany) with 5x magnification in the reflected light mode was employed to obtain the reference measurements of coating thickness. After the tablets were measured using 3D OCT, they were cut with a scalpel on one side and then broken. Since smearing of the coating by the blade affected the readings, the broken side was analyzed. The coating thickness was determined by averaging 5 positions measured close to the apex using the vendor software (Leica Application Suite v4.9). The error introduced by the manual identification of the interface was estimated to be 5 µm for a single reading. The estimate was based on the interpretation of the same microscopy image by different operators.

3. Results

3.1. PLS model for NIR spectroscopy

Both, for off-line and at-line applications, a PLS model was developed to predict the coating thickness, with a mean diameter gain per sample as the reference. Since the presentation of the tablets to the probe was very different, two PLS models were required. Off-line tablets were in direct contact with the probe, while for at-line measurement there was a distance between them of about 5 mm, leading to lower intensity captured by the probe and noisier spectra. The spectra were pretreated with SNV in a spectral range of 1200–2030 nm, and the PLS model was developed in the same range. A coating specific peak was observed at 1394 nm. Samples from coating time 0 min (uncoated cores) were excluded from the PLS model due to the distinct differences in surface scattering properties of the tablet core and the coated tablet. Additionally, uncoated cores are commonly prone to attrition, which leads to a reduction in weight and dimension (detailed in discussion section). Both PLS models consisted of 3 latent variables. The PLS metrics were $R^2 = 0.87$, RMSEP = 7.8 µm and $Q^2 = 0.83$, RMSECV = 8.7 µm for off-line and $R^2 = 0.89$, RMSEP = 7.2 µm and $Q^2 = 0.81$, RMSECV = 9.1 µm for at-line.

3.2. Refractive index for OCT

Unfortunately, materials databases do not list the wavelength-dependent refractive index n of complex multi-component and multi-phase media (e.g., coating polymer with plasticizer and anti-tacking agent). This refractive index is required to translate the OCT pixel count into absolute coating thickness values. For a measured pixel count p, an image height z_{air}, a total number of pixels p_{total} of 1024, the coating thickness d is determined via $d = \frac{pz_{air}}{p_{total}n}$. We compared three approaches to determine n of the coating: (1) a direct measurement of the coating thickness via light microscopy imaging of broken tablets, (2) a calculation of coating thickness based on the measured weight gain and (3) a calculation of n based on a volume-weighted mixture of the coating components' refractive indices. As described below, in the first two methods n was calculated to match the measured coating thicknesses. In the third method n was calculated based on literature values. The results are summarized in Table 1. The impact on the determined coating thickness is notable. A coating which has 100 µm at $n = 1.37$, at a given OCT pixel count, has 92.7 µm for $n = 1.27$ and 109.3 µm for $n = 1.498$, varying nearly by ± 10%.

The coating thickness of 10 tablets after 240 min of coating time was analyzed using the light microscope. Only tablets with a clean breakage line were compared. Prior to breaking the tablets, OCT measurements were performed in similar positions.

The second method for determining n was to calculate the coating thickness via the average weight gain of 100 tablets for coating times of 45–240 min. The first minutes of coating were excluded due to unknown attrition of the tablet core. The density of dry coating mass was calculated to be $\rho = 1.465\,g/cm^3$.

Lastly, n was calculated using values n_D of the raw materials reported in the literature. These literature values are measured at 589 nm, at the sodium D-line. Since the refractive index is typically wavelength-dependent (see Cauchy or Sellmayr equation of dispersion), it is slightly different at 830 nm, which is the central wavelength of OCT.

Table 1
Overview of refractive indices determined.

Approach	*n*
Light microscopy	1.37 ± 0.07
Weight gain	1.27 ± 0.11
Volume weighted mixture	1.498

All calculations required significant simplifications: the solvent is fully evaporated, the coating is free of pores, the coating solution is perfectly mixed and no coating solution diffuses into the tablet core. These assumptions are most likely not valid for real coatings. A minimum level of diffusion into the core is required to bond the coating to the core. Excess diffusion can cause a multitude of effects: the solvent may remain in the core leading to a higher residual moisture and weight and, potentially, to a swelling of the core. Additionally, coating solution that migrated into the table core does not contribute to the function of the coating, e.g., enteric protection. Light microscopy provided the only direct thickness measurement, and thus we used $n = 1.37$ in all subsequent analysis.

3.3. Off-line method comparison

The five methods, i.e., OCT, NIR, and weight-, height- and diameter-gain, were compared in terms of (1) repeatability, (2) influence on the tablet core, (3) coating thickness variation on a single tablet and (4) resulting coating thickness variation between the tablets. A summary of the results is provided in Table 2.

First, the repeatability of each method was evaluated by performing ten replicate measurements of a single tablet (sample 165 min, tablet #4). Since for NIR and OCT the tablet was not moved between the measurements, these methods measured the effect of sensor noise on the PLS model prediction and image analysis, respectively.

Next, the influence of the tablet core properties for NIR and weight-, height- and diameter-gain was assessed by calculating the SD of ten tablet cores. Generally for OCT, swelling or attrition of the tablet core (changes in the core dimensions during coating) does not influence the coating thickness reading. However, the tablet's core roughness can influence the distribution of coating thicknesses on a tablet. The coating layer itself can have an additional thickness variability due to the statistical nature of the coating process. The core roughness affects the coating thickness and its distribution (*intra*-tablet variation). Especially with regard to OCT, the *intra*-tablet variation refers to the coating quality and is not a measurement error. It was assessed by calculating the SD of coating thickness in 3D OCT scans, consisting of 512B-scans, of three tablets (sample 165 min, tablet #4 - #6).

Lastly, the *inter*-tablet variation was evaluated. To that end, 10 labelled tablets per sample, as described in Section 2.2, were examined via all five methods. In Table 2, the *inter*-tablet variability was calculated as the SD of the mean-centered data for all samples drawn at 45 min until the end of the process. Before 45 minutes of coating the layer thickness was below the limit of detection for OCT. As such, the SD reflects both the coating thicknesses and the measurement accuracy. In this case, both in-line methods, i.e., OCT and NIR, showed the lowest SDs, followed by the diameter-gain.

The results of coating thickness measurements and the corresponding *inter*-tablet SDs of all five methods for the drawn samples are shown in Fig. 1. The data was pretreated in order to highlight the correlations between the methods and to remove the obvious correlation of coating thickness gain due to the coating progress. For each method and sample (i.e., tablets drawn at the same time from the process) the measurements of the ten tablets were mean-centered. For example, the mean weight gain of the ten tablets drawn at 135 min was subtracted from the individual weight gain measurements at 135 min.

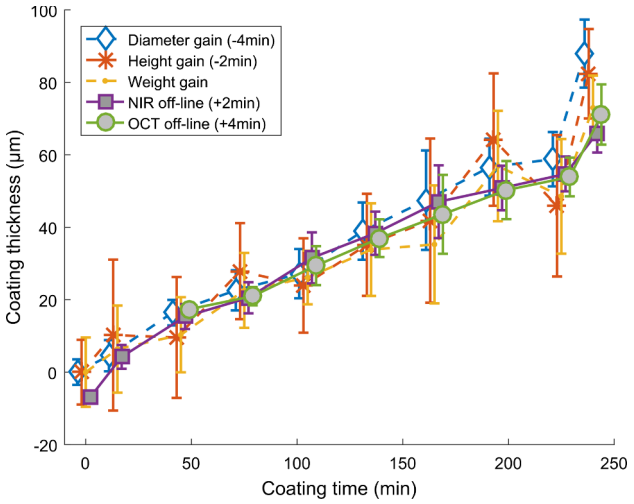

Fig. 1. The growth of the coating thickness over coating time, as measured by all five methods. For a better visualization of all curves, the data points are shifted up to four minutes from the original sampling time (see legend).

A graphical matrix of the correlations consisting of the scatter plots of two methods as well as Pearson's correlation coefficients ρ are shown in Fig. 2. Here, all drawn samples from coating time 45 min until the process end at 240 min are considered. The methods diameter gain, NIR and OCT all correlate strongly to each other (> 0.80). Moreover, height gain and weight gain correlate at the same level (0.84) to each other but poorly to the other methods (diameter-gain, NIR and OCT). A correlation between the height and weight can be expected since heavier tablets are thicker at a constant bulk density. The poor correlation to the other methods can be attributed to significant height and weight variations in the tablet core (see Table 2). This is probably due to fluctuations in the powder flow into the die of the tablet press, leading to varying dosed volumes or powder densities prior to compaction. The resulting weight and height variations are also reflected in a broader distribution, as shown in the histograms of Fig. 2.

As Fig. 1 indicates, at 165 min of coating time the variation between all methods for the sample is the highest. This is the reason why this sample was examined in more detail. Fig. 3 presents the coating thicknesses of ten tablets, as determined via all methods. Three tablets (#4 - #6) with a pronounced variation are highlighted with black filled circles. Their corresponding OCT images are shown in Fig. 4 and the coating thicknesses are summarized in Table 3. The cross-sectional images visually confirm the reported high *inter*-tablet coating thickness variations. Interestingly, the top, bottom and band of a single tablet have consistent coating thicknesses. The low *intra*-tablet variability is confirmed via OCT 3D mapping of the top and bottom in an area of 6.12 mm × 6.12 mm.

In summary, the analysis on coating thickness *intra*- and *inter*-tablet homogeneity show very different outcomes. The width of the mean-

Table 2
Overview of the off-line method comparison results. Details on the samples used to calculate each column are in the main text. (1) Ten replicate measurements without moving the tablet (2) could be determined via NIR-chemical imaging (not part of this study) and (3) 3D OCT measurement of top and bottom of three tablets.

	Repeatability SD (µm)	Tablet core SD (µm)	*Intra*-tablet variation (µm)	*Inter*-tablet variation (µm)
Weight gain	± 0.0000 mg	± 2.0 mg/ ± 9.6 µm	N.A.	12.0
Height gain	± 2.4	± 8.9	N.A.	15.8
Diameter gain	± 3.3	± 3.5	N.A.	7.9
NIR	± 0.1 (1)	± 1.7	N.A. (2)	5.9
OCT	± 0.0 (1)	N.A.	± 2.8 (3)	6.3

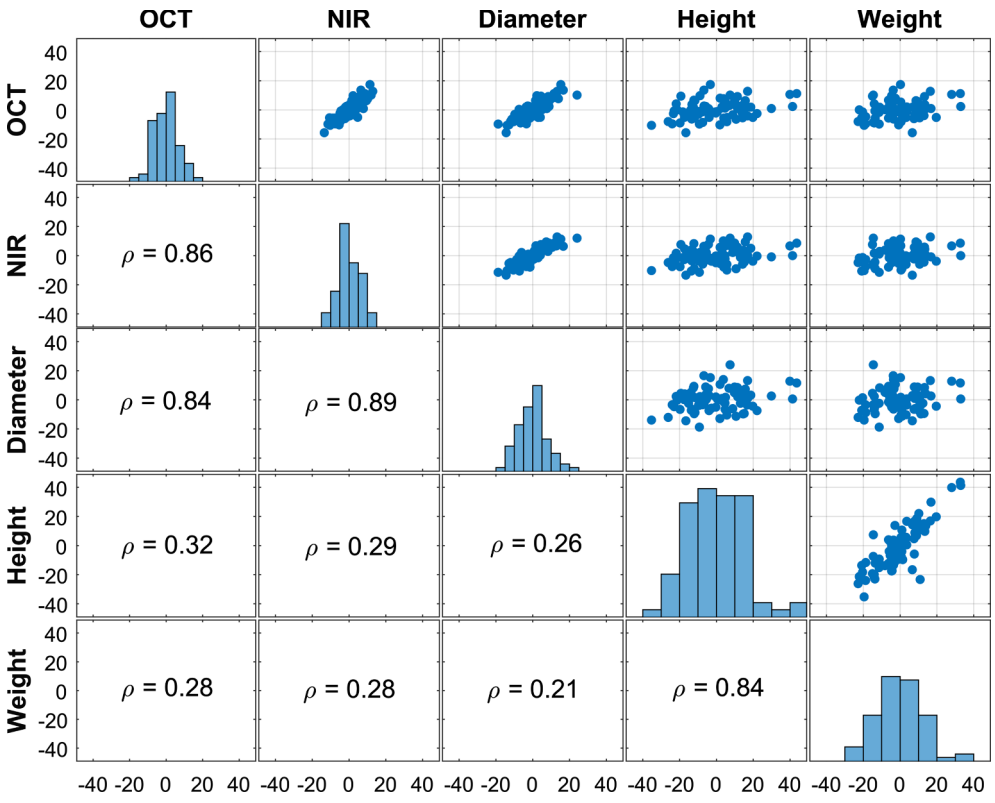

Fig. 2. Visualization of the correlation between the methods for all samples from coating time 45 min until the process end at 240 min. Both axis show mean-centered coating thicknesses (µm) of the various methods plotted against each other. The histograms show the distribution for a single method. Below the diagonal of the matrix the Pearson correlation coefficient ρ between the respective methods are shown.

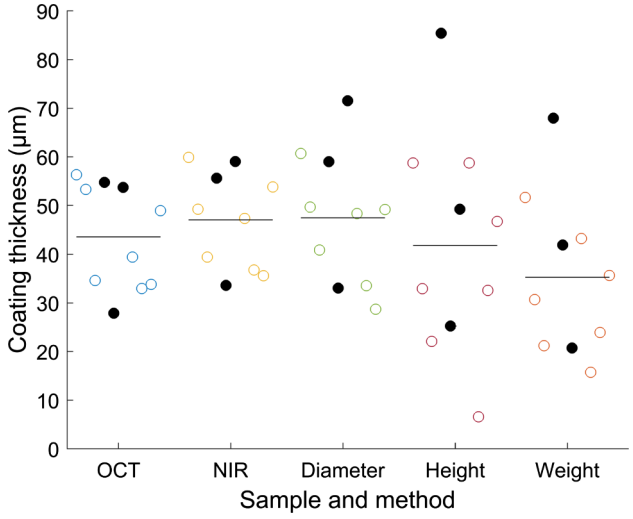

Fig. 3. Coating thickness of 10 tablets from the sample at 165 min of process time. The black lines show the mean value for each method. The black-filled circles are tablets #4 – #6, as shown in Fig. 4.

centered coating thickness data, as shown in Fig. 1, shows that the tablets have a large *inter*-tablet variability. Despite that, the *inter*-tablet variability, as shown via OCT cross-sectional images in Fig. 4 is low.

In literature one study of tablet dimension measurements stated that the coating thickness variation between the top and the band depends strongly on the tablet shape, with round tablets having the lowest variation [32]. Another study that applied terahertz on round tablets, reported a pronounced difference between top/bottom and band [33]. The literature and our results suggest, that shape is only one of many influential factors for coating homogeneity. Thus, minimizing *inter*- and *intra*-coating variability is a multivariate optimization task.

3.4. At-line measurements via in-line capable methods

For at-line measurement all approx. 150 to 200 drawn tablets from a sample were measured at once in the sampling device. Typical NIR spectra and OCT images are presented in Fig. 5. The NIR spectra for all sampling times shown were averaged per sample, after removing the non-tablet spectra. The OCT images shown in the Figure are for a sample at 240 min of coating time.

The analyzed results are shown in Fig. 6, comparing at-line and previously discussed off-line data for both methods. As can be clearly seen, the gain of coating thickness is detected by both methods (Fig. 6, left). Interestingly, both technologies have the same pattern of offset between off-line and at-line (see Fig. 6, right), except at 165 minutes when the number of NIR spectra after sorting was significantly lower (by a factor of 2 - 3) than in the other samples. It is likely that the NIR probe was not ideally positioned in that case. The synchronized variation of the offset (at-line vs. off-line) between NIR and OCT confirmed the good correlation between the methods (although the reason for this offset is not known). Additionally, due to a higher number of samples measured at-line, the measured mean value is expected to be closer to the mean value of the entire sample than that of 10 tablets analyzed off-line. The SD of the at-line data is in the same range as off-line, i.e., for OCT 5.8 µm at-line and 6.3 µm off-line, as well as 6.1 µm at-line and 5.9 µm off-line for NIR. The SD was calculated for the samples at 45 min to the end of the process.

Additional information about the surface roughness and homogeneity index was obtained via OCT (see Fig. 7) as this is the only method that can provide such data. Interestingly, the surface roughness and its SD increased during the coating process. In our previous work, we could show that, compared to the tablet core, the surface roughness increased over process time [31]. No clear trend was established for the homogeneity index, a measure for the fraction of scattering areas in the coating. Towards the process end, the homogeneity of samples stayed nearly constant. In other words, regardless of the coating thickness, the appearance of layers in terms of “dark spots” remained the same.

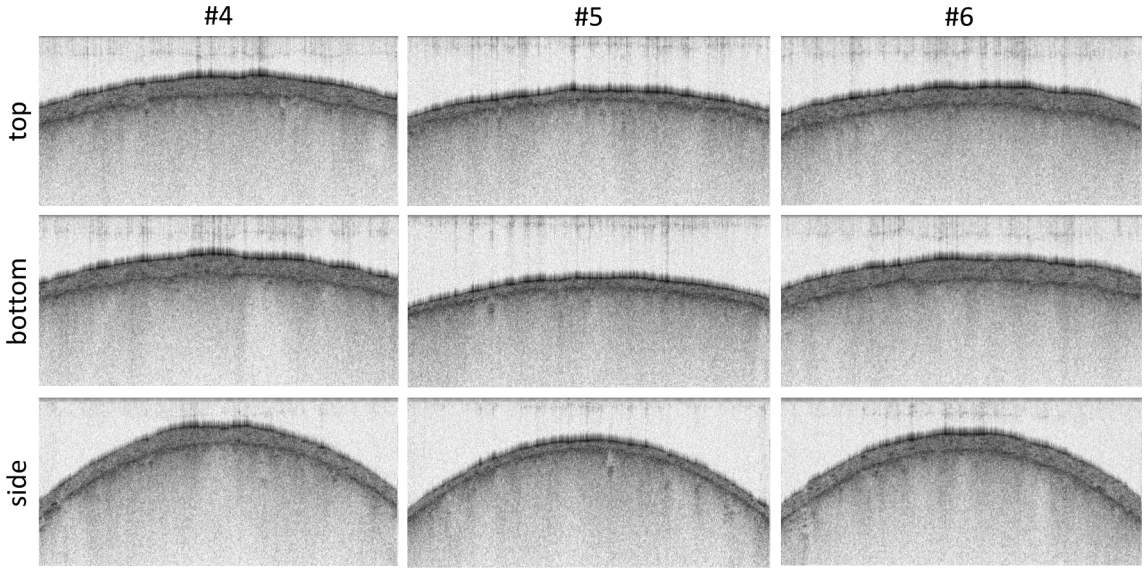

Fig. 4. OCT cross-sectional images of the top, bottom and band of tablet numbers 4 to 6. The tablets are from the sample at 165 min of process time.

Table 3
3D OCT results for 3 tablets, shown in Fig. 4. The scanned area is 6.12 × 6.12 mm, consisting of 1024 × 512 A-scans.

Tablet	#4	#5	#6
Top (μm)	49.8 ± 2.9	25.5 ± 2.1	51.8 ± 3.8
Bottom (μm)	51.1 ± 2.8	25.4 ± 2.4	53.0 ± 3.0
Band (μm)	51.3 ± 4.6	28.6 ± 3.0	53.0 ± 3.1

4. Discussion

4.1. Off-line measurements

Coating recipes in pharmaceutical manufacturing are currently based on weight gain. Our current study demonstrates that weight gain is a poor measure of coating thickness. For single tablets, it correlates poorly with the diameter-gain, NIR and OCT (Pearson's correlation coefficients of $\rho < 0.3$), primarily due to significant deviations in the tablet core weight, compared to the low weight of the coating. In this case, a high precision of the balance has no benefits. Typically, a high SD in the core weight is compensated by relying on the statistics of large sample sizes and on sampling several hundred tablets for weight gain. Yet this method provides no information on the coating thickness distribution between the tablets. Other influential factors are the potential swelling of the core due to water uptake and attrition of the tablet core in the beginning of the coating process, which would lead to a bias. The water uptake bias can be prevented by determining loss-on-drying (LoD) before and after coating, while the attrition bias cannot be determined by weight measurements only.

The weight-gain method has the advantage of directly determining the coating efficiency by comparing the dry mass of applied coating solution to the weight gain. The disadvantages of this approach are the necessary correction of the weight gain for the tablet core moisture uptake and the remaining bias in terms of attrition. OCT and NIR data plotted over diameter gain (from 45 minutes to process end) were fit with a first order polynomial in order to estimate the attrition. Where the fit intersects 0 μm, the diameter gain was −6.7 μm and −7.9 μm for OCT and NIR, respectively. Thus, attrition is likely to be in this range.

The height-gain results were similarly affected by the tablet core variability. An increase in the core tablet weight results in an increased height at equal bulk density. This is also reflected by correlation factors $\rho = 0.84$ between the height- and weight-gain methods. The variation in the tablet core height was higher by nearly a factor of four than the error of the manual caliper measurement.

Based on the results of this study, OCT, NIR and diameter-gain are

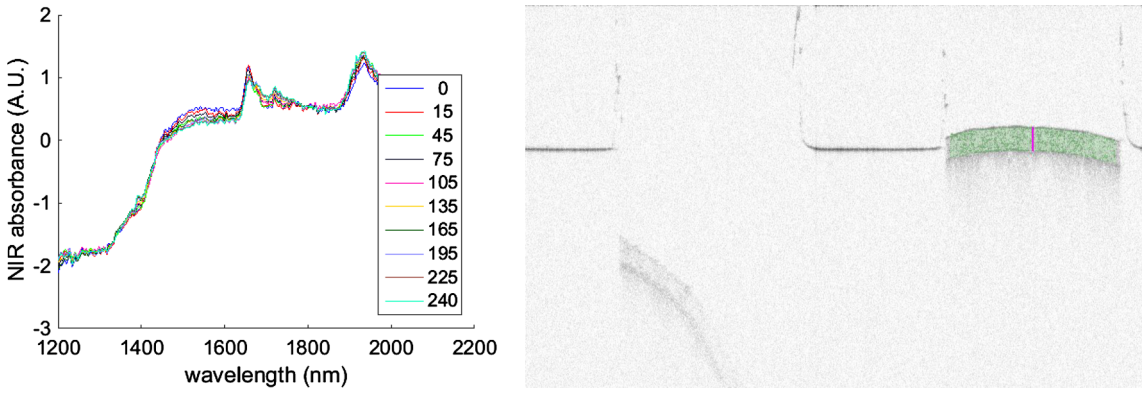

Fig. 5. Left: Averaged NIR spectra for each sample after removing the non-tablet spectra. Right: OCT image of the sample at t = 240 min. The green area highlights the detected layer and the vertical violet line indicates the mean coating thickness. (For interpretation of the references to colour in this figure legend, the reader is referred to the web version of this article.)

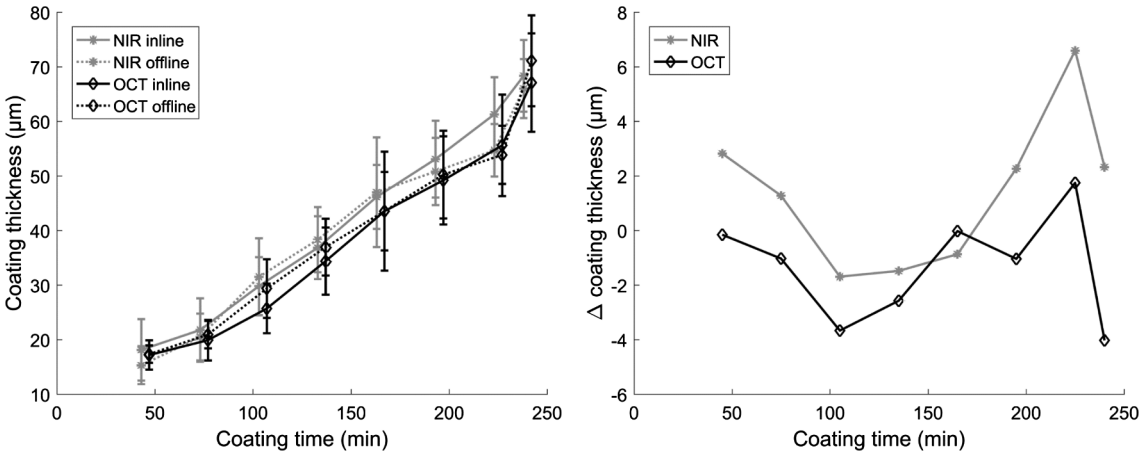

Fig. 6. Comparison between at-line (dotted line) and off-line (solid line) results for NIR (circle) and OCT (diamond). Left: Absolute coating thicknesses over process time. Right: coating thickness difference between at-line and off-line results over process time.

more precise methods for measuring the coating thickness, with a very good correlation ($\rho > 0.8$) between all three methods for single tablets. Since the NIR model was calibrated with the diameter gain as reference data, a strong correlation was expected. OCT was referenced independently via light microscopy and correlated equally well. This suggests that all three methods measured the same property.

The diameter of tablet cores is well-defined by the punch geometry of the tablet press and has a much lower variance than the height and weight. Therefore, the main source of variation is the manual caliper measurement. Other influential factors are possible swelling and attrition.

Since OCT directly measures the coating thickness based on the optical path length, the coating thickness obtained is not affected by swelling and attrition. The 2D cross-sectional images (see Fig. 4 and Table 3) illustrate a strong variation in the mean coating thickness of up to 30 µm for tablets from a single sample. The *intra*-tablet coating variability of 2.9 µm for these samples was an order of magnitude smaller. This indicates that the coating thickness for this specific setup has a good *intra*-tablet uniformity but a poor *inter*-tablet uniformity.

The NIR signal is a volume-based average spectrum of the chemical composition of penetrated volume. An increase in the spectral contribution of the coating material was calibrated against diameter gain. The NIR result is independent on dimensional changes of the tablet core, but can be influenced by the moisture uptake since water has a pronounced NIR signal. This increases the modelling effort but offers insights into the residual moisture after coating.

4.2. At-line measurements

At-line measurement of coating thickness of single tablets in a setup which mimics an in-line process interface was possible via both OCT and NIR methods. The SD of the at-line data is in the same range as the off-line data for both NIR and OCT, and the absolute coating thickness values are comparable. This suggests that both methods delivered consistent results. Hence, both methods fulfill an important goal of developing an in-line method: achieving comparable accuracy and precision with the off-line method.

For at-line application of NIR spectra, sorting had to be performed to remove spectra for instances when no tablet was in front of the sensor. Additionally, since the process interface (distance probe to tablet) was different from that off-line, a new calibration model had to be developed. Although a greater distance also led to noisier spectra, no significant effect on the prediction quality was observed.

For at-line application of OCT, no modifications of software or hardware are necessary. What is more, OCT provide information beyond coating thickness. An increased roughness over the coating time that was observed (Fig. 7, left) which may be due to mechanical forces in the pan coater or the coating droplet deposition during the coating process. Since the mechanical forces acting on the tablets increase with the tablet bed height, roughness can also be a good indicator for scale-up. The homogeneity index (Fig. 7, right) was nearly constant towards the process end. This suggests that the coating conditions, such as solvent evaporation rate, bed and air temperature, spray rates and

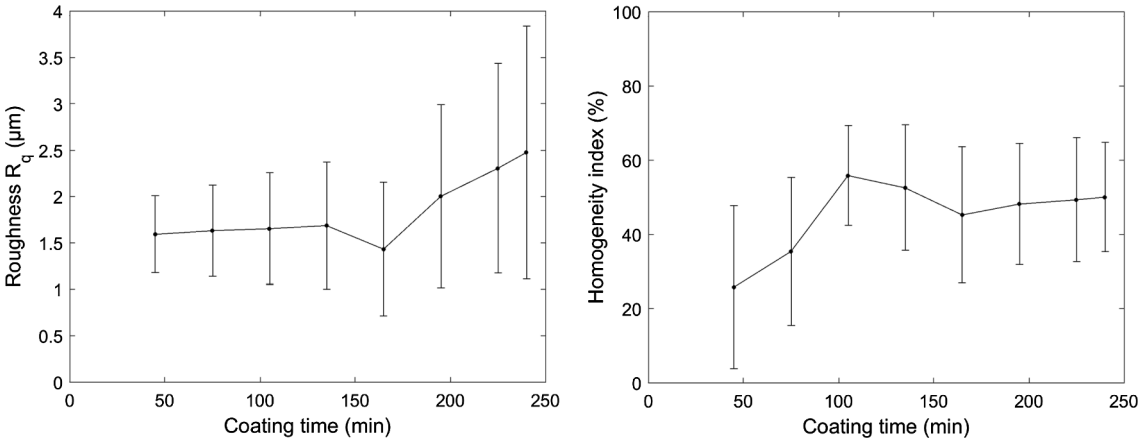

Fig. 7. At-line OCT results for surface roughness (left) and homogeneity index (left) over process time.

coating solution properties, were constant during the entire process. Most importantly, OCT does not require extensive model development as needed using NIR spectroscopy, instead a simpler referencing based on determining the refractive index of the examined material is used.

4.3. Summary

From the methods compared, diameter-gain, OCT and NIR showed consistent results, which correlated well to each other. OCT and NIR at-line and off-line performance was comparable. The effort for the method development and transfer to at-line application was significantly smaller for OCT, since it directly measures the coating thickness, while chemometric modeling is required for NIR measurements. Due to a large number of samples measured at-line, the measured mean value and SD are expected to be closer to the mean coating thickness values of the entire sample (or batch) than those obtained based on the ten tablets analyzed off-line. This is reflected by the coating growth over time: the at-line approaches had smaller deviations from a linear growth than the off-line reference methods. As such, the coating thickness variation determined via in-line methods is a statistically more correct representation of the entire batch. The data clearly supports the statement that in-line methods surpass conventional off-line reference methods.

When comparing OCT and NIR to the diameter-gain method, attrition was estimated to be in the range of 6.7 µm (via OCT) and 7.9 µm (via NIR), leading to a small weight loss and reduced dosage strength. This weight loss is not taken into account in the coating efficiency calculations. Hence, the actual coating efficiency will be higher and more coating suspension is deposited on the tablets, contributing to the coating thickness. Different levels of attrition of the tablet core in the beginning of the process, in addition to commonly considered spray drying and turbulent air flow, may be a notable contribution to the coating-efficiency differences between coaters. Therefore, next to achieving a low *inter*-tablet coating uniformity, a second optimization opportunity is to reduce the forces acting on the tablet core until a sufficient protective coating layer has formed.

A broad distribution of coating thicknesses was observed. Even at the end of coating process, with a mean coating thickness of about 70 µm, the *inter*-tablet SD was about 9 µm or 13% RSD. This indicates that the tablets had a broad distribution of spray zone passes. The *intra*-tablet homogeneity of 2.9 µm, as measured via 3D OCT, was comparably low. Hence, the tablets in the spray zone had no preferred orientation. This information is valuable for process development since it indicates that a broad distribution in the number of spray zone passes is the root cause of the coating thickness variations observed.

Further research could be directed towards the functional performance of coatings. The coating functionality is likely to be determined not only by its thickness. For controlled release coatings, the link has to be established between the dissolution rate and the coating thickness and its variability, yet also including OCT parameters, such as surface roughness and homogeneity index. Furthermore, understanding how the coating process affects these parameters could provide important information about the coating.

Acknowledgements

This work was funded by the Austrian COMET Program under the auspices of the Austrian Federal Ministry of Transport, Innovation and Technology (bmvit), the Austrian Federal Ministry of Economy, Family and Youth (bmwfj) and by the State of Styria (Styrian Funding Agency SFG). COMET is managed by the Austrian Research Promotion Agency FFG.

References

[1] K. Knop, P. Kleinebudde, PAT-tools for process control in pharmaceutical film coating applications, Int. J. Pharm. 457 (2013) 527–536, https://doi.org/10.1016/j.ijpharm.2013.01.062.
[2] F. Siepmann, J. Siepmann, M. Walther, R.J. MacRae, R. Bodmeier, Polymer blends for controlled release coatings, J. Contr. Rel. 125 (2008) 1–15, https://doi.org/10.1016/J.JCONREL.2007.09.012.
[3] R. Langer, New methods of drug delivery, Science 80 (249) (1990) 1527–1533, https://doi.org/10.1126/science.2218494.
[4] R.K. Verma, B. Mishra, S. Garg, Osmotically controlled oral drug delivery, Drug Dev. Ind. Pharm. 26 (2000) 695–708, https://doi.org/10.1081/DDC-100101287.
[5] P. Boehling, G. Toschkoff, S. Just, K. Knop, P. Kleinebudde, A. Funke, H. Rehbaum, P. Rajniak, J.G. Khinast, Simulation of a tablet coating process at different scales using DEM, Eur. J. Pharm. Sci. 93 (2016) 74–83, https://doi.org/10.1016/j.ejps.2016.08.018.
[6] S. Just, G. Toschkoff, A. Funke, D. Djuric, G. Scharrer, J. Khinast, K. Knop, P. Kleinebudde, Optimization of the inter-tablet coating uniformity for an active coating process at lab and pilot scale, Int. J. Pharm. 457 (2013) 1–8, https://doi.org/10.1016/j.ijpharm.2013.09.010.
[7] N.A. Peppas, B. Narasimhan, Mathematical models in drug delivery: how modeling has shaped the way we design new drug delivery systems, J. Contr. Rel. 190 (2014) 75–81, https://doi.org/10.1016/j.jconrel.2014.06.041.
[8] E. Kaunisto, M. Marucci, P. Borgquist, A. Axelsson, Mechanistic modelling of drug release from polymer-coated and swelling and dissolving polymer matrix systems, Int. J. Pharm. 418 (2011) 54–77, https://doi.org/10.1016/J.IJPHARM.2011.01.021.
[9] M. Andersson Trojer, L. Nordstierna, M. Nordin, M. Nydén, K. Holmberg, Encapsulation of actives for sustained release, Phys. Chem. Chem. Phys. 15 (2013) 17727, https://doi.org/10.1039/c3cp52686k.
[10] M. Wolfgang, P. Wahl, S. Sacher, E. Gartshein, J.G. Khinast, Real-time measurement of coating film thickness, Pharm. Technol. 43 (2019) 36–47.
[11] M. Kumpugdee-Vollrath, J.-P. Krause, eds., Easy Coating, Vieweg + Teubner, Wiesbaden, 2011. doi:10.1007/978-3-8348-9896-8.
[12] P. Boehling, G. Toschkoff, K. Knop, P. Kleinebudde, S. Just, A. Funke, H. Rehbaum, J.G. Khinast, Analysis of large-scale tablet coating: modeling, simulation and experiments, Eur. J. Pharm. Sci. 90 (2016) 14–24, https://doi.org/10.1016/J.EJPS.2015.12.022.
[13] J. Wang, J. Hemenway, W. Chen, D. Desai, W. Early, S. Paruchuri, S.-Y. Chang, H. Stamato, S. Varia, An evaluation of process parameters to improve coating efficiency of an active tablet film-coating process, Int. J. Pharm. 427 (2012) 163–169, https://doi.org/10.1016/J.IJPHARM.2012.01.033.
[14] S. Porter, G. Sackett, L. Liu, Development, Optimization, and Scale-Up of Process Parameters, Dev. Solid Oral Dos. Forms, Elsevier, 2017, pp. 953–996, , https://doi.org/10.1016/B978-0-12-802447-8.00034-0.
[15] K. Korasa, G. Hudovornik, F. Vrečer, Applicability of near-infrared spectroscopy in the monitoring of film coating and curing process of the prolonged release coated pellets, Eur. J. Pharm. Sci. 93 (2016) 484–492, https://doi.org/10.1016/J.EJPS.2016.08.038.
[16] S.H. Tabasi, R. Fahmy, D. Bensley, C. O'Brien, S.W. Hoag, Quality by design, part II: application of NIR spectroscopy to monitor the coating process for a pharmaceutical sustained release product, J. Pharm. Sci. 97 (2008) 4052–4066, https://doi.org/10.1002/jps.21307.
[17] C. Gendre, M. Genty, M. Boiret, M. Julien, L. Meunier, O. Lecoq, M. Baron, P. Chaminade, J.M. Péan, Development of a process analytical technology (PAT) for in-line monitoring of film thickness and mass of coating materials during a pan coating operation, Eur. J. Pharm. Sci. 43 (2011) 244–250, https://doi.org/10.1016/j.ejps.2011.04.017.
[18] P. Avalle, M.J. Pollitt, K. Bradley, B. Cooper, G. Pearce, A. Djemai, S. Fitzpatrick, Development of process analytical technology (PAT) methods for controlled release pellet coating, Eur. J. Pharm. Biopharm. 87 (2014) 244–251, https://doi.org/10.1016/J.EJPB.2014.01.008.
[19] J.D. Pérez-Ramos, W.P. Findlay, G. Peck, K.R. Morris, Quantitative analysis of film coating in a pan coater based on in-line sensor measurements, AAPS PharmSciTech 6 (2005) E127–E136, https://doi.org/10.1208/pt060120.
[20] J. Müller, D. Brock, K. Knop, J. Axel Zeitler, P. Kleinebudde, Prediction of dissolution time and coating thickness of sustained release formulations using Raman spectroscopy and terahertz pulsed imaging, Eur. J. Pharm. Biopharm. 80 (2012) 690–697, https://doi.org/10.1016/J.EJPB.2011.12.003.
[21] M. Wirges, A. Funke, P. Serno, K. Knop, P. Kleinebudde, Development and in-line validation of a process analytical technology to facilitate the scale up of coating processes, J. Pharm. Biomed. Anal. 78–79 (2013) 57–64, https://doi.org/10.1016/J.JPBA.2013.01.037.
[22] H. Lin, Y. Dong, D. Markl, B.M. Williams, Y. Zheng, Y. Shen, J.A. Zeitler, Measurement of the intertablet coating uniformity of a pharmaceutical pan coating process with combined terahertz and optical coherence tomography in-line sensing, J. Pharm. Sci. 106 (2017) 1075–1084, https://doi.org/10.1016/J.XPHS.2016.12.012.
[23] C. Pei, H. Lin, D. Markl, Y.-C. Shen, J.A. Zeitler, J.A. Elliott, A quantitative comparison of in-line coating thickness distributions obtained from a pharmaceutical

tablet mixing process using discrete element method and terahertz pulsed imaging, Chem. Eng. Sci. 192 (2018) 34–45, https://doi.org/10.1016/J.CES.2018.06.045.
[24] N. Oman Kadunc, R. Šibanc, R. Dreu, B. Likar, D. Tomaževič, In-line monitoring of pellet coating thickness growth by means of visual imaging, Int. J. Pharm. 470 (2014) 8–14, https://doi.org/10.1016/J.IJPHARM.2014.04.066.
[25] S. García-Muñoz, D.S. Gierer, Coating uniformity assessment for colored immediate release tablets using multivariate image analysis, Int. J. Pharm. 395 (2010) 104–113, https://doi.org/10.1016/J.IJPHARM.2010.05.026.
[26] D. Markl, M. Zettl, G. Hannesschläger, S. Sacher, M. Leitner, A. Buchsbaum, J.G. Khinast, Calibration-free in-line monitoring of pellet coating processes via optical coherence tomography, Chem. Eng. Sci. 125 (2015) 200–208, https://doi.org/10.1016/j.ces.2014.05.049.
[27] D. Markl, G. Hannesschäger, S. Sacher, M. Leitner, A. Buchsbaum, R. Pescod, T. Baele, J.G. Khinast, In-line monitoring of a pharmaceutical pan coating process by optical coherence tomography, J. Pharm. Sci. 104 (2015) 2531–2540, https://doi.org/10.1002/jps.24531.
[28] D. Oelkrug, M. Brun, K. Rebner, B. Boldrini, R. Kessler, Penetration of light into multiple scattering media: model calculations and reflectance experiments. Part I: the axial transfer, Appl. Spectrosc. 66 (2012) 934–943, https://doi.org/10.1366/11-06518.
[29] O. Scheibelhofer, P.R. Wahl, B. Larchevêque, F. Chauchard, J.G. Khinast, Spatially resolved spectral powder analysis: experiments and modeling, Appl. Spectrosc. 72 (2018) 521–534, https://doi.org/10.1177/0003702817749839.
[30] J.A. Zeitler, Y. Shen, C. Baker, P.F. Taday, M. Pepper, T. Rades, Analysis of coating structures and interfaces in solid oral dosage forms by three dimensional terahertz pulsed imaging, J. Pharm. Sci. 96 (2007) 330–340, https://doi.org/10.1002/jps.20789.
[31] D. Markl, P. Wahl, H. Pichler, S. Sacher, J.G. Khinast, Characterization of the coating and tablet core roughness by means of 3D optical coherence tomography, Int. J. Pharm. 536 (2018) 459–466, https://doi.org/10.1016/j.ijpharm.2017.12.023.
[32] K.E. Wilson, E. Crossman, The influence of tablet shape and pan speed on intra-tablet film coating uniformity, Drug Dev. Ind. Pharm. 23 (1997) 1239–1243, https://doi.org/10.3109/03639049709146164.
[33] L. Ho, R. Müller, K.C. Gordon, M. Pepper, T. Rades, Y. Shen, P.F. Taday, J.A. Zeitler, Terahertz pulsed imaging as an analytical tool for sustained-release tablet film coating, Eur. J. Pharm. Biopharm. 71 (2009) 117–123, https://doi.org/10.1016/J.EJPB.2008.06.023.